Robust Motion Control of a Linear Motor Positioner Using Fast Nonsingular Terminal Sliding Mode

Jinchuan Zheng, *Member, IEEE*, Hai Wang, *Member, IEEE*, Zhihong Man, *Member, IEEE*, Jiong Jin, *Member, IEEE*, and Minyue Fu, *Fellow, IEEE*

***Abstract*—A robust motion control system is essential for the linear motor (LM)-based direct drive to provide high speed and high-precision performance. This paper studies a systematic control design method using fast nonsingular terminal sliding mode (FNTSM) for an LM positioner. Compared with the conventional nonsingular terminal sliding mode control, the FNTSM control can guarantee a faster convergence rate of the tracking error in the presence of system uncertainties including payload variations, friction, external disturbances, and measurement noises. Moreover, its control input is inherently continuous, which accordingly avoids the undesired control chattering problem. We further discuss the selection criteria of the controller parameters for the LM to deal with the system dynamic constraints and performance tradeoffs. Finally, we present a robust model-free velocity estimator based on the only available position measurements with quantization noises such that the estimated velocity can be used for feedback signal to the FNTSM controller. Experimental results demonstrate the practical implementation of the FNTSM controller and verify its robustness of more accurate tracking and faster disturbance rejection compared with a conventional NTSM controller and a linear H_∞ controller.**

***Index Terms*—Linear motor (LM), motion control, robust control, terminal sliding mode (TSM).**

I. Introduction

LINEAR motor (LM)-based direct drives are widely used in high-speed and high-precision motion control systems since they eliminate the mechanical transmission problems such as backlash, friction, and structural resonances. The applications of LMs to positioning systems include the machine tool direct feed drive [1]–[3], dual-stage positioning stage [4], industrial gantry [5], high-speed XY table [6], and so on.

With the ever increasing use of LMs in higher precision industrial machines, the demand for higher performance LMs continues to increase as well. Hence, on one hand, researchers have attempted to redesign the LM structure with respect to its mechanism or electronics for improved dynamic characteristics and for the ease of control. For example, a new permanent-magnet LM was proposed in [7] by using a nine-pole ten-slot structure and a proper winding method, which was shown to effectively reduce the cogging force by 90%. Recently, Sato also reported a linear synchronous motor design with moving permanent magnet [8]; and it was demonstrated that the prototype can achieve a much higher thrust density for ultrahigh acceleration over 100 G and velocity than conventional drives. On the other hand, extensive research efforts have been devoted to the control methods for the LMs to achieve the desired performance. This is because the feedback control, as compared to the open-loop control, has been widely recognized as being able to provide more accurate and reliable performance. Moreover, on LM direct drive systems both the payload variations and the disturbances such as frictions from the guideways or cutting forces in machine tools, are directly acting on the LM itself, making the motion precision more likely to be deteriorated. This further explains the importance of the motion controller for the LMs to ensure the performance and robustness. For this purpose, a variety of control techniques have been developed, for example, relay control for ripple and friction compensation [9], multirate control [10], adaptive control for cogging force compensation [5], iterative learning control [11], H_∞ optimal control [1], [12], nonlinear control for reduced settling time [4], and nonlinear robust control using sliding mode [13]–[15], which we will also focus on in this paper.

Sliding mode control (SMC) is a systematic and effective approach to robust control that maintains the system stability and consistent performance in the presence of modeling uncertainties and disturbances. Furthermore, it allows a design tradeoff between tracking performance and smoothing control discontinuity for practical implementation on most applications [16]. The SMC has been successfully applied to a lot of mechatronic systems such as hard disk drive [17], permanent-magnet synchronous motor [18], steer-by-wire system on vehicles [19], and robotic hands [20]. The fundamental design procedure of the SMC is to properly design a stable sliding surface s, which satisfies the desired specifications, and then, select a feedback control law u (typically discontinuous) such that the sliding surface could be reached and retained in the sense of Lyapunov, despite the presence of modeling uncertainties and disturbances [16]. Since the designs of both sliding surface and control law are not unique for a given control problem, a number of design methods have been proposed since the initial idea of SMC began in the late 1950s. A complete survey of these methods is introduced in [21] and [22] and references therein. Among these methods, the so-called terminal sliding mode (TSM) control [23] proposed a nonlinear sliding surface design that guarantees the reachability of the sliding mode $s = 0$ in finite time. This is a

Manuscript received April 30, 2014; revised July 1, 2014; accepted August 24, 2014. Date of publication September 11, 2014; date of current version August 12, 2015. Recommended by Technical Editor M. O. Efe.

J. Zheng, H. Wang, Z. Man, and J. Jin are with the School of Software and Electrical Engineering, Swinburne University of Technology, Hawthorn, Vic. 3122, Australia (e-mail: jzheng@swin.edu.au; wanghai0652@gmail.com; zman@swin.edu.au; jiongjin@swin.edu.au).

M. Fu is with the School of Electrical Engineering and Computer Science, The University of Newcastle, Callaghan, N.S.W. 2308, Australia (e-mail: Minyue.Fu@newcastle.edu.au).

Color versions of one or more of the figures in this paper are available online at http://ieeexplore.ieee.org.

Digital Object Identifier 10.1109/TMECH.2014.2352647

significant improvement compared with the conventional SMC of linear sliding surface, which only ensures asymptotical convergence of s [16]. Moreover, a discrete-time TSM controller was proposed in [24] from the discrete-time point of view, which was more practical for real-time implementation. To avoid the singularity problem of control input associated with the TSM, a nonsingular terminal sliding mode (NTSM) control method was then presented in [25], which simply swaps the state variables in the conventional TSM function while retaining the finite-time convergence feature. However, the control discontinuity problem still exists in the NTSM although it was recommended in [25] that the boundary layer method [16] could be adopted to reduce the undesired chattering of the discontinuous control. Alternatively, adaptive SMC [26] was proposed to reduce the amplitude of chattering for systems whose parameters or disturbances are slowly time varying. Recently, a new design method [27] named as fast nonsingular terminal sliding mode (FNTSM) control in this paper, was proposed to overcome the disadvantages of the NTSM. The FNTSM control law involves no switching elements, and thus, avoids the control chattering in essence. Moreover, it incorporates an effective control law in the reaching phase by using the fast-TSM-type model [28] such that the exponential stability as well as faster finite-time convergence than the NTSM control can be achieved. Motivated by these benefits, we thus apply the FNTSM control technique to a real LM positioner system and experimentally investigate its design method and implementation, which is still rare in the literature of the high-precision LM motion control.

In this paper, we first present the plant model of the LM setup and its parametric uncertainties. Particularly, we formulate the mass variations due to payload as multiplicative uncertainty that can lead to a less conservative bound of the tracking error as compared with the additive form of mass uncertainty in [27]. Next, we develop an FNTSM controller for the LM with the proof showing its capability to drive the tracking error to converge to a bounded region in finite time. Moreover, we discuss the selection criteria of the controller parameters in terms of system dynamic constraints and performance tradeoffs. Because in our setup the position of the LM stage is the only measurement for feedback control, we further design a sliding-mode-based velocity estimator [29], which is shown to obtain robust velocity estimation performance against the quantization noise from the position measurements as well as velocity frequency changes. Finally, we implement the FNTSM controller on the real LM setup. The experimental results are shown to verify its superior performance in terms of more accurate tracking and faster disturbance rejection over a conventional NTSM controller and a linear H_∞ controller.

This paper is organized as follows. Section II presents the plant model with the parametric uncertainties on the LM system under study. The FNTSM control design method is described in Section III where the selection criteria of the controller parameters are discussed in details and a robust velocity estimator is also presented for practical implementation of the state-feedback based controller. Finally, Section IV presents the experimental results to verify the effectiveness of the FNTSM controller. Section V concludes this paper.

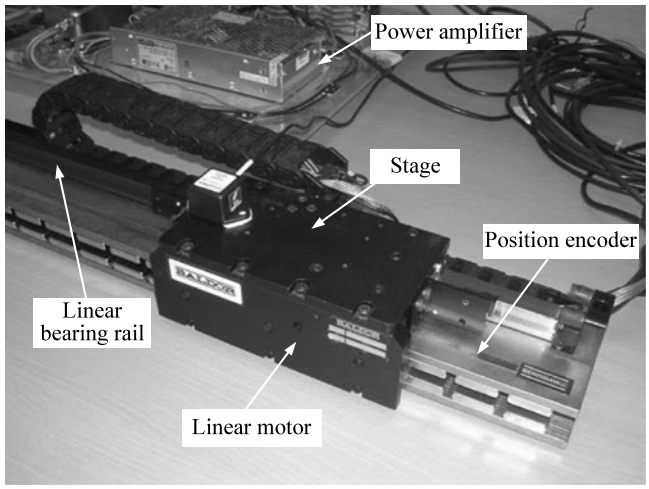

Fig. 1. Experimental setup of an LM positioner control system.

II. Plant Modeling

The experimental setup for the LM positioner system (by Baldor Electric Company) is shown in Fig. 1. The positioning stage is directly driven by an LM, which has a 500-mm travel range and is equipped with a position encoder (by Renishaw PLC) of a resolution of 1 μm. The voltage-to-current power amplifier is used to convert the control input signals into current commands to drive the LM. In our setup, the power amplifier has a bandwidth of 400-Hz, which is much higher than that of the LM dynamics. Thus, its model is simply regarded as a constant gain.

In [30], we have reported a complete mathematical model for the LM system. To proceed with the control design, we shall give the plant model of the LM as follows:

$$\begin{cases} m\ddot{y} = u - f - d \\ f = k_v\dot{y} + k_c\mathrm{sgn}(\dot{y}) \end{cases} \tag{1}$$

where y represents the position of the stage, u is the control input, f is the friction force, d is the lumped uncertainties including disturbance, measurement noise, and unmodeled system dynamics, m is the moving mass of the positioner, k_v is the viscous friction coefficient, k_c is the Coulomb friction level, and $\mathrm{sgn}(\cdot)$ denotes the standard signum function.

In this paper, we consider the parametric uncertainty as follows:

$$\begin{aligned} \frac{1}{\tau} \le \frac{m}{m_0} &\le \tau \quad (m_0 = 3.31 \text{ kg}, \ \tau = 2) \\ |k_v - k_{v0}| &\le \bar{k}_v \quad (k_{v0} = 8.6 \text{ Ns/m}, |\bar{k}_v| = 1) \\ |k_c - k_{c0}| &\le \bar{k}_c \quad (k_{c0} = 11.5 \ N, \ |\bar{k}_c| \le 3) \\ |d| &\le \bar{d} \quad (\bar{d} = 15) \end{aligned} \tag{2}$$

where m_0, k_{v0}, and k_{c0} denote the nominal model parameters, and τ, $\bar{k}_v$, $\bar{k}_c$, and $\bar{d}$ are the bounds of the uncertain parameters, respectively. In particular, τ is also called the gain margin of the control system because it measures the robustness of the control law with respect to the control gain [16].

Define δ as

$$\delta = (k_v - k_{v0})\dot{y} + (k_c - k_{c0})\mathrm{sgn}(\dot{y}) + d. \tag{3}$$

Then, we have

$$|\delta| \le \bar{\delta} = \bar{k}_v|\dot{y}| + (\bar{k}_c + \bar{d}). \tag{4}$$

III. Control Design

Our control objective here is to design a robust controller such that the LM positioner can track a reference command fast and accurately in the presence of the model uncertainties and disturbances. To achieve this goal, we will first present a controller design method using FNTSM. It will be seen that the FNTSM controller is constructed with the LM velocity as feedback signals, which is, however, not measurable in our setup. Hence, we will then present a robust model-free velocity estimator to estimate the velocity from the position measurements that are contaminated by quantization noises.

A. FNTSM Controller for LM

Define the tracking error as

$$e = y - y_r \tag{5}$$

where y_r is the reference command supposed to be twice differentiable. Furthermore, define a sliding variable s as

$$s = e + \lambda \mathrm{sig}(\dot{e})^{\gamma} \tag{6}$$

where $\lambda > 0$, $1 < \gamma < 2$, and the notation $\mathrm{sig}(x)^a$ as first introduced in [31] is a simplified expression of

$$\mathrm{sig}(x)^a = |x|^a \mathrm{sgn}(x). \tag{7}$$

Note that the function $\mathrm{sig}(x)^a$, for $a > 0$ $\forall x \in R$ is smooth and monotonically increasing and always returns a real number. Furthermore, according to [25], we know that the TSM function as defined by

$$s = e + \lambda \mathrm{sig}(\dot{e})^{\gamma} = 0 \tag{8}$$

for any initial conditions of $e(0)$ and $\dot{e}(0)$ can converge to zeroes in a finite time t_s given by

$$t_s = \frac{\lambda^{-\frac{1}{\gamma}}}{1 - \frac{1}{\gamma}} |e(0)|^{1 - \frac{1}{\gamma}}. \tag{9}$$

Next, we shall derive an expression of u_0, i.e., the so-called equivalent control input [16], which would maintain

$$\dot{s} = \dot{e} + \lambda\gamma|\dot{e}|^{\gamma - 1}(\ddot{y} - \ddot{y}_r) = 0 \tag{10}$$

if the plant model is in the absence of uncertainties. More specific, let the model parameters in (1) be their nominal values and suppose $d = 0$, and replace u by u_0. Then, solving (10) for u_0 by using the nominal plant model leads to

$$u_0 = m_0\ddot{y}_r + k_{c0}\mathrm{sgn}(\dot{y}) + k_{v0}\dot{y} - \frac{m_0}{\lambda\gamma}\mathrm{sig}(\dot{e})^{2-\gamma}. \tag{11}$$

Furthermore, we introduce a reaching control input u_1 given by

$$u_1 = -m_0[k_1 s + k_2 \mathrm{sig}(s)^{\rho}] \tag{12}$$

where $k_1, k_2 > 0$, $0 < \rho < 1$, and the sliding variable s is with (6).

Now, we have the following theorem regarding the form of the FNTSM controller.

Theorem 1: Consider the LM system in (1) with the parametric uncertainties in (2). Then, under the FNTSM control law

$$u = u_0 + u_1 \tag{13}$$

where u_0, u_1 is with (11), (12), respectively, the following tracking performance can be guaranteed.

(1) The sliding variable s converges to the region of

$$|s| \le \Phi = \min(\Phi_1, \Phi_2) \tag{14}$$

$$\Phi_1 = \frac{(\tau - 1)|\ddot{y}_r - \frac{1}{\lambda\gamma}\mathrm{sig}(\dot{e})^{2-\gamma}| + \frac{1}{m_0}\bar{\delta}}{k_1} \tag{15}$$

$$\Phi_2 = \left[\frac{(\tau - 1)|\ddot{y}_r - \frac{1}{\lambda\gamma}\mathrm{sig}(\dot{e})^{2-\gamma}| + \frac{1}{m_0}\bar{\delta}}{k_2}\right]^{\frac{1}{\rho}} \tag{16}$$

in a finite time, where $\bar{\delta}$ is given in (4).

(2) As a result of *1*), the tracking error e and its velocity $\dot{e}$ converge to the region of

$$\begin{aligned} |e| &\le 2\Phi \\ |\dot{e}| &\le \left(\tfrac{\Phi}{\lambda}\right)^{\frac{1}{\gamma}} \end{aligned} \tag{17}$$

in a finite time.

Proof: Choose the Lyapunov function $V = \frac{1}{2}s^2$. Evaluating the derivative of V along the trajectories of the system in (1) with u in (13) yields

$$\dot{V} = \Gamma s - \Psi_1 s^2 - \Psi_2 |s|^{\rho + 1} \tag{18}$$

with

$$\begin{aligned} \Gamma &= \left(\frac{m_0}{m} - 1\right)(\lambda\gamma|\dot{e}|^{\gamma - 1}\ddot{y}_r - \dot{e}) - \frac{1}{m}\lambda\gamma|\dot{e}|^{\gamma - 1}\delta \\ \Psi_1 &= \frac{m_0}{m}\lambda\gamma|\dot{e}|^{\gamma - 1}k_1 \\ \Psi_2 &= \frac{m_0}{m}\lambda\gamma|\dot{e}|^{\gamma - 1}k_2. \end{aligned} \tag{19}$$

It is obvious that the last two terms in (18) are both nonnegative and the term Γ stems from the system uncertainties, namely, we can see from (19) that Γ reduces to zero in the absence of uncertainties. Next, we shall derive the condition for (18) to satisfy the finite-time stability [32]. There exist two different cases.

Case 1) Rewrite (18) as the following form:

$$\dot{V} = -\left(\Psi_1 - \frac{\Gamma}{s}\right)s^2 - \Psi_2|s|^{\rho + 1}. \tag{20}$$

Hence, if $\dot{e} \neq 0$ and $\Psi_1 - \frac{\Gamma}{s} > 0$, then there exists $\varepsilon_1,\ \varepsilon_2 > 0$ such that

$$\begin{aligned} \dot{V} &\le -\varepsilon_1 s^2 - \varepsilon_2|s|^{\rho + 1} \\ &= -2\varepsilon_1 V - 2^{\frac{\rho + 1}{2}}\varepsilon_2 V^{\frac{\rho + 1}{2}} \end{aligned} \tag{21}$$

which apparently leads to the finite-time stability (see the Appendix). Furthermore, the convergence time can be

obtained as

$$t_r \leq \frac{1}{(1-\rho)\varepsilon_1}\ln\left[1+\frac{\varepsilon_1}{\varepsilon_2}(2V_0)^{\frac{1-\rho}{2}}\right] \tag{22}$$

where $V_0 = V(s(0))$ is the initial condition.

From the aforementioned analysis, to achieve the property of finite-time stability, we shall proceed to find the region of s that guarantees $\Psi_1 - \frac{\Gamma}{s} > 0$, which can actually result from

$$|s| > \frac{|\Gamma|}{\Psi_1} = \frac{\left|\left(1-\frac{m}{m_0}\right)\left[\ddot{y}_r - \frac{1}{\lambda\gamma}\mathrm{sig}(\dot{e})^{2-\gamma}\right] - \frac{1}{m_0}\delta\right|}{k_1}. \tag{23}$$

Using the bounds of the system uncertainties, we have

$$\frac{|\Gamma|}{\Psi_1} \leq \frac{(\tau-1)|\ddot{y}_r - \frac{1}{\lambda\gamma}\mathrm{sig}(\dot{e})^{2-\gamma}| + \frac{1}{m_0}\bar{\delta}}{k_1} = \Phi_1. \tag{24}$$

Therefore, the condition $\Psi_1 - \frac{\Gamma}{s} > 0$ is guaranteed only if

$$|s| > \Phi_1. \tag{25}$$

In other words, the region

$$|s| \leq \Phi_1 \tag{26}$$

can be reached under the FNTSM control law in a finite time as given by (22).

Case 2) Alternatively, rewrite (18) as the following form:

$$\dot{V} = -\Psi_1 s^2 - \left[\Psi_2 - \frac{\Gamma}{\mathrm{sig}(s)^\rho}\right]|s|^{\rho+1}. \tag{27}$$

Similarly, letting $\Psi_2 - \frac{\Gamma}{\mathrm{sig}(s)^\rho} > 0$, for $\dot{e} \neq 0$ suffices to achieve the finite time stability of V. Hence, performing the similar analysis as that in *Case 1* yields the region given by

$$|s| \leq \Phi_2 = \left[\frac{(\tau-1)|\ddot{y}_r - \frac{1}{\lambda\gamma}\mathrm{sig}(\dot{e})^{2-\gamma}| + \frac{1}{m_0}\bar{\delta}}{k_2}\right]^{\frac{1}{\rho}} \tag{28}$$

which can also be reached under the FNTSM control law in a finite time.

Finally, we shall show that $\dot{e} = 0$ for the aforementioned two cases is not an attractor in the reaching phase. Substituting (13) into (1) for $\dot{e} = 0$ yields

$$\ddot{e} = \left(\frac{m_0}{m} - 1\right)\ddot{y}_r - \frac{\delta}{m} - \frac{m_0}{m}[k_1 s + k_2 \mathrm{sig}(s)^\rho]. \tag{29}$$

Then, for any $\dot{e} = 0$, we have

$$\ddot{e} = \begin{cases} -\dfrac{m_0}{m}\left[k_1 - \dfrac{\left(1-\frac{m}{m_0}\right)\ddot{y}_r - \frac{1}{m_0}\delta}{s}\right]s - \dfrac{m_0}{m}k_2\mathrm{sig}(s)^\rho \\ \qquad\qquad \neq 0, \quad \text{for } |s| > \Psi_1, \\ -\dfrac{m_0}{m}k_1 s - \dfrac{m_0}{m}\left[k_2 - \dfrac{\left(1-\frac{m}{m_0}\right)\ddot{y}_r - \frac{1}{m_0}\delta}{\mathrm{sig}(s)^\rho}\right]\mathrm{sig}(s)^\rho \\ \qquad\qquad \neq 0, \quad \text{for } |s| > \Psi_2 \end{cases}$$

which implies $\dot{e} = 0$ is not an attractor for $|s| > \Psi_1$ or $|s| > \Psi_2$. Hence, for $\dot{e} = 0$, the finite-time reachability of s can also be guaranteed.

By far, combining the results in (26) and (28) yields that the sliding variable s under the FNTSM control law in (13) can converge to the region with $|s| \leq \Phi = \min(\Phi_1, \Phi_2)$ in a finite time.

To get the result of (17), rewrite (6) as

$$e + \left[\lambda - \frac{s}{\mathrm{sig}(\dot{e})^\gamma}\right]\mathrm{sig}(\dot{e})^\gamma = 0. \tag{30}$$

Then, letting $|\dot{e}| > (\frac{\Phi}{\lambda})^{\frac{1}{\gamma}}$ implies $\lambda - \frac{s}{\mathrm{sig}(\dot{e})^\gamma} > 0$ since $|s| \leq \Phi$. As such, the function (30) keeps the same property of finite-time stability as that in (8), which reversely means that the velocity of tracking error converges to the region

$$|\dot{e}| \leq \left(\frac{\Phi}{\lambda}\right)^{\frac{1}{\gamma}} \tag{31}$$

in a finite time. Accordingly, from (30), we can deduce that the tracking error converges to the region

$$|e| \leq \lambda|\dot{e}|^{\frac{1}{\gamma}} + |s| \leq 2\Phi. \tag{32}$$

in a finite time as well. The proof is thus completed.

Remark 1: By expressing the perturbed mass m as the bounded multiplicative uncertainty in (2) instead of the additive form [27], we have a tighter bound of the uncertainty, which consequently leads to less conservative bounds of the convergence regions in (15) and (16).

Remark 2: To compare the benefits of FNTSM control with the conventional NTSM control, we also present the form of a conventional NTSM controller based on the boundary layer method as follows:

$$u_N = u_0 - m_0 k_2 \mathrm{sat}\left(\frac{s}{\Delta}\right) \tag{33}$$

where s, u_0, and k_2 are the same as those in (6), (11), and (12), respectively, for a fair comparison; $\mathrm{sat}(x)$ is the saturation function defined as $\mathrm{sat}(x) = \mathrm{sgn}(\cdot)\min\{1, |x|\}$, which replaces the original signum function to reduce the control chattering; and Δ is the boundary layer thickness. It has been reported in [25] that the tracking error under the NTSM control law (33) will also converge to the bounded region given by

$$|s| \leq \Delta \Rightarrow |e| \leq \Delta \tag{34}$$

in the finite time

$$t_r^* < \frac{|s(0)|}{k_2}. \tag{35}$$

Apparently, the NTSM controller (33) can be approximated from the FNTSM controller (13) by setting $k_1 = 0$ and $\rho = 0$.

Remark 3: The FNTSM control law is substantially continuous (i.e., chattering free) and singularity free, and therefore, it could be easily implemented on the real LM system. Furthermore, for a nominal LM system, the FNTSM control can still guarantee the tracking error to converge to zero in a finite time, which can be seen from (14) by setting $\tau = 1$ and $\bar{\delta} = 0$. Comparatively, the NTSM control law can eliminate control chattering by choosing a sufficiently thick boundary layer. However, for the nominal system, it can only guarantee that the tracking

error converges into the boundary layer rather than zero in a finite time [27].

Remark 4: Comparing the convergence time under the FNTSM (22) with that under the NTSM (35), we can see that the FNTSM has a faster convergence rate because of its implied exponential stability. This means that the FNTSM control can settle the tracking error significantly faster than the NTSM in the presence of an external shock disturbance as will be demonstrated in Fig. 9 later.

B. Selection of Controller Parameters

To this end, we have shown that the FNTSM control has several advantages over the conventional NTSM control. However, without exception, the selection of its controller parameters should be carefully investigated when practically applied to the LM because the ideal tracking performance is generally compromised with measurement noise characteristics, limited control efforts, and particularly, with unmodeled system dynamics.

1) Selection of λ*:* The parameter λ critically determines the control bandwidth of the sliding mode dynamics as can be implied from (8). Clearly, a smaller λ leads to a larger bandwidth, indicating a faster response speed and higher tracking accuracy. However, the minimum λ applicable to our case is dominated by the measurement noises (detailed in Section III-C) and the time delay associated with the LM. More specific, the experimental frequency response of the LM system as we reported in [4] has shown that the LM dynamics are affected by continuous phase drops (equivalent to a time delay) from 50 Hz relative to its rigid-body model. After evaluation of these factors, we choose a $\lambda = 0.016$ in practical implementation.

2) Selection of γ*:* The defined range with $1 < \gamma < 2$ avoids the singularity problem [25] of the control input, which can be seen from the last term in (11). From the point of view of the performance, a larger γ leads to a smaller convergence time (9) but at the cost of amplifying the velocity measurement noises (or estimation errors), which may consequently introduce extra control chattering in u_0 (11). Hence, we choose $\gamma = 1.4$.

3) Selection of ρ*:* Compared with the standard NTSM control without using the boundary layer [25], the index ρ is introduced to eliminate the control chattering. We can observe from (12) that a larger ρ in $(0,\ 1)$ leads to a smoother control signal u_1 but at the cost of weaker robustness. From the actual implementation, a value of $\rho = 0.8$ shows an acceptable balance between robustness and control smoothness.

4) Selections of k_1 *and* k_2*:* The positive gains k_1 and k_2 can be made either constant or time varying. Implied by the results in (14)–(17), we intuitively choose

$$k_1 = 5 \times 10^4 \left[(\tau - 1)|\ddot{y}_r - \frac{1}{\lambda\gamma}\mathrm{sig}(\dot{e})^{2-\gamma}| + \frac{1}{m_0}\bar{\delta} \right]$$

$$k_2 = 650 \left[(\tau - 1)|\ddot{y}_r - \frac{1}{\lambda\gamma}\mathrm{sig}(\dot{e})^{2-\gamma}| + \frac{1}{m_0}\bar{\delta} \right]$$

so as to easily predict the bound of the tracking error, i.e., $40\ \mu$m for these selections.

C. Velocity Estimator

It can be seen from (11) and (12) that the FNTSM controller relies on both the position and velocity of the LM as feedback signals. However, in our setup, only the position measurement is available. Hence, a velocity estimator is essential for practical implementation of the controller. There have a variety of state estimation approaches reported in the literature such as the well-known Luenberger observer, Kalman filter, and their many variations [33]. The accuracy of these estimators generally depends on the extent to which the exact information of the plant model is known. However, this is not applicable in our case where the LM contains nontrivial uncertainties. Thus, a model-free velocity estimator is more suitable for our application also because velocity is naturally the differentiation of position signals.

For this goal, the backward differentiator (BD) is the most popular model-free velocity estimator due to its simplicity, which is given by

$$\hat{\dot{y}}_{\mathrm{BD}}(n) = \frac{y_m(n) - y_m(n-1)}{T_s} \tag{36}$$

where $\hat{\dot{y}}_{\mathrm{BD}}(n)$ is the estimated velocity at the time step n, y_m is the measured position signal, and T_s is the sampling period. Note that the measured position signal y_m contains quantization noise due to the employed position encoder [30], which when differentiated would induce significant estimation error. Recall that the measurement noise including the velocity estimation error is involved in the lumped uncertainty d in (1). It can be seen from (4) that a higher level measurement noise causes a larger bound of the uncertainty $\bar{\delta}$, which in turn results in a larger tracking error according to (14)–(17). Moreover, the measurement noise may also introduce extra chattering in the control input signal as can be seen from (11) and (12). Such control chattering may excite the unmodeled system dynamics and deteriorate the tracking performance.

To effectively reduce the velocity estimation error, we adopt a model-free robust exact differentiator (RED) using sliding mode technique [29]. The structure of the RED is given by

$$\begin{aligned} \hat{\dot{y}}_{\mathrm{RED}} &= z - \eta_1 |\hat{y} - y_m|^{\frac{1}{2}} \mathrm{sgn}(\hat{y} - y_m) \\ \dot{z} &= -\eta_2 \mathrm{sgn}(\hat{y} - y_m) \end{aligned} \tag{37}$$

where $z \in R$ is an auxiliary state variable, $\hat{\dot{y}}_{\mathrm{RED}}$ is the estimated velocity, and $\eta_1, \eta_2 > 0$. It was proved in [29] that the velocity estimation error under the RED (37) can converge to the region

$$|\hat{\dot{y}}_{\mathrm{RED}} - \dot{y}| < \sigma\nu^{\frac{1}{2}}$$

in a finite time, where $\dot{y}$ is the actual velocity, $\sigma > 0$ is a constant determined by η_1 and η_2, and ν is the quantization noise level.

To verify the velocity estimation performance by using BD and RED, we carry out comparative simulations, where the estimator parameters are chosen as $T_s = 0.2$ ms, $\eta_1 = 2.25$, and $\eta_2 = 0.0023$, respectively. Moreover, we use a first-order low-pass filter with cut-off frequency 100 Hz to further smooth the estimated velocities of each estimator. The results are presented in Fig. 2, where the top plot shows the actual position signal y with varying frequencies, and the position measurement with a

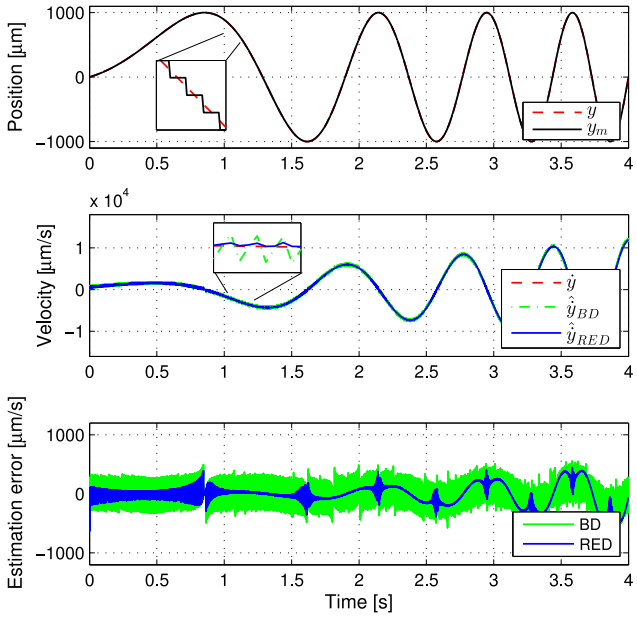

Fig. 2. Comparison of velocity estimation performance using BD and RED.

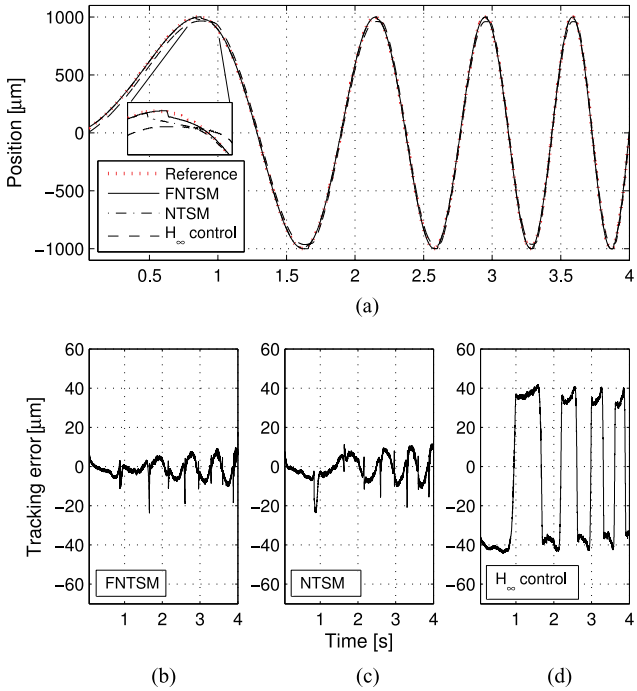

Fig. 3. Tracking responses to a swept sinusoidal reference without payload. (a) Position profiles; and tracking errors of (b) FNTSM, (c) NTSM, (d) H_∞ control.

quantization noise level 0.5 μm (i.e., half of the position encoder resolution). The middle plot shows the estimated velocity signals from y_m. We can see from the bottom plot that the estimation error obtained by RED is significantly smaller than that by BD, and this benefit is robust along the velocity profile with different frequencies. However, the RED still contains a small level of errors due to the fact that it is impossible to eliminate them completely in practice. As such, when the RED is applied to the FNTSM controller, these errors will induce a certain level of tracking error and chattering in the control input as will be seen from the experimental results in the next section.

IV. Experimental Results

To verify the performance of the designed FNTSM controller with the velocity estimator using RED, experiments are conducted on the real LM positioner system. For comparison, we also carry out the experiments, respectively, under the presented conventional NTSM controller (33) by setting $\Delta = 40$, and under a linear H_∞ controller

$$u_H = 3.31\ddot{y}_r + 8.6\dot{y} - 3.27 \times 10^5 e - 2112\dot{e}. \quad (38)$$

Note that the H_∞ controller is designed based on a state-space approach as given in [1], which guarantees an optimal bounded tracking error for the uncertainties among all the linear state-feedback controllers.

All the designed controllers were implemented on a real-time DSP system (dSPACE-DS1103) with the sampling period of 0.2 ms.

A. Swept Sinusoidal Tracking Performance and Robustness

We first evaluate the tracking performance in response to a swept sinusoidal reference of an amplitude of 1000 μm and whose frequency varies linearly with time from 0.5 to 1.0 Hz. Fig. 3 shows the time responses of the position profiles and tracking errors under the three controllers without extra payloads applied to the LM stage. We can see that the FNTSM controller achieves the smallest tracking error bound (TEB), i.e., $\max(|e|) = 24$ μm, along the profile, which is only 2.4% of the reference amplitude. In this case, the tracking error profile under the NTSM controller is close to that under FNTSM. Note that the obtained TEBs under the FNTSM and NTSM are consistent with the initial designs that aim for $|e| < 40$ as can be seen from (17) and (34), respectively. Comparatively, the H_∞ controller has the largest TEB and tends to induce more oscillations when the reference frequency increases indicating a common feature of the linear control. Among the controllers, the maximum tracking errors that exhibit as spikes/jumps all occur at the points where the reference velocity changes its sign, e.g., at $t = 0.86$ s. These errors are mainly caused by the insufficient compensation for the friction force, which results from the difficulty of estimating velocity accurately from quantized position measurements at the zero crossing of velocity (see Fig. 2). Fig. 4 also shows the reasonably smooth control input signals under the FNTSM and NTSM except a small amount of chattering due to the measurement noises.

To further verify the robustness against the payload change, we place a 3.5-kg payload on the LM stage, i.e., making $\frac{m}{m_0} \approx 2$. We can see from the results in Fig. 5 that the FNTSM and NTSM both maintain the tracking performance properly, but the H_∞ controller gets worse performance with a larger TEB of 50 μm as compared with the result of 44 μm without payload in Fig. 3(d). Moreover, the control input signals as shown in Fig. 6 indicate that the H_∞ controller contains larger oscillations

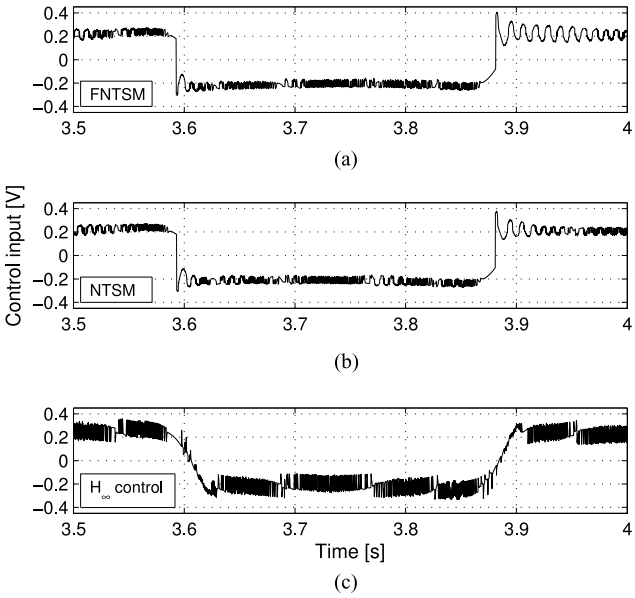

Fig. 4. Control input responses to a swept sinusoidal reference without payload. (a) FNTSM; (b) NTSM; (c) H_∞ control.

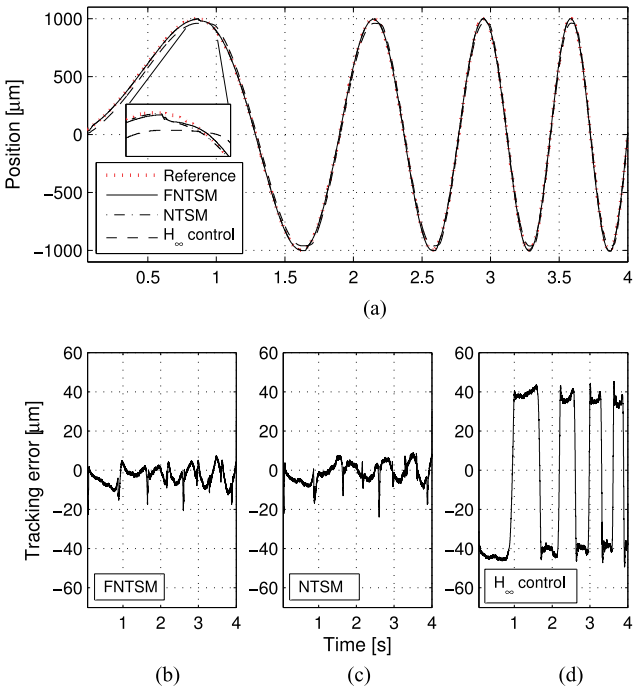

Fig. 5. Tracking responses to a swept sinusoidal reference with payload. (a) Position profiles; and tracking errors of (b) FNTSM, (c) NTSM, (d) H_∞ control.

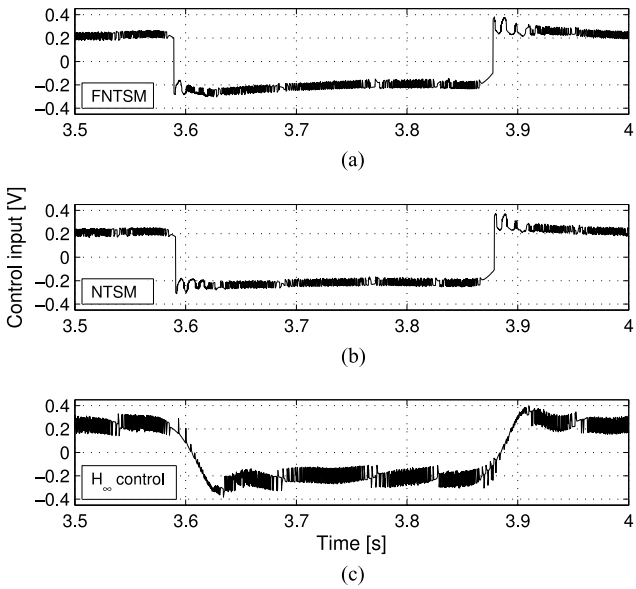

Fig. 6. Control input responses to a swept sinusoidal reference with payload. (a) FNTSM; (b) NTSM; (c) H_∞ control.

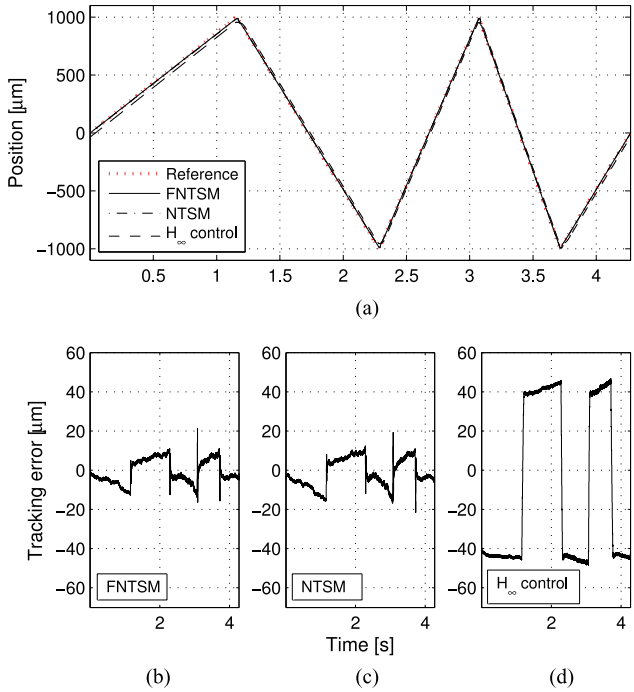

Fig. 7. Tracking responses to a slope-varying triangular reference without payload. (a) Position profiles; and tracking errors of (b) FNTSM, (c) NTSM, (d) H_∞ control.

(e.g., at $t = 3.9$ s) because of its decreased stability margin with the applied payload.

B. Triangular Tracking Performance and Robustness

Next, we evaluate the tracking performance in response to another commonly used reference, i.e., a slope-varying triangular waveform of an amplitude of 1000 μm. Not surprisingly, the results in Figs. 7 and 8 show that the FNTSM controller achieves the best performance in the case either without payload or with payload in comparison with those under NTSM and H_∞ control. This verifies that the FNTSM can maintain the tracking performance and robustness against different types of references as well.

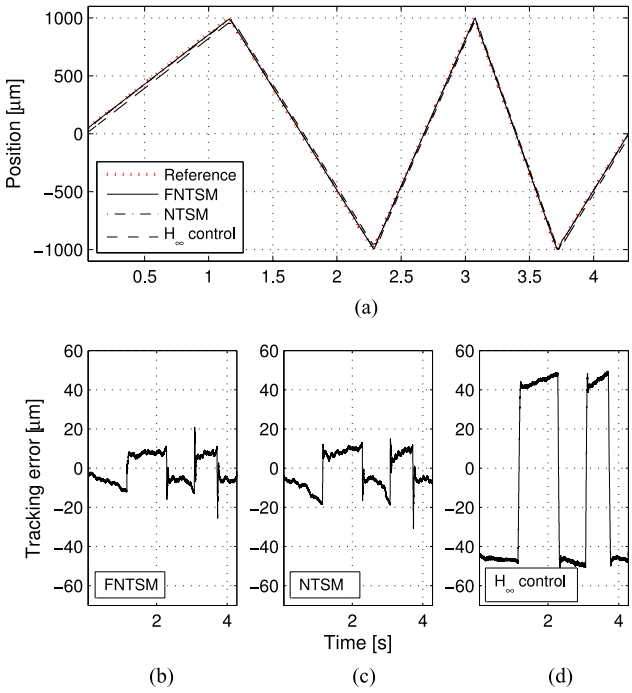

Fig. 8. Tracking responses to a slope-varying triangular reference with payload. (a) Position profiles; and tracking errors of (b) FNTSM; (c) NTSM; (d) H_∞ control.

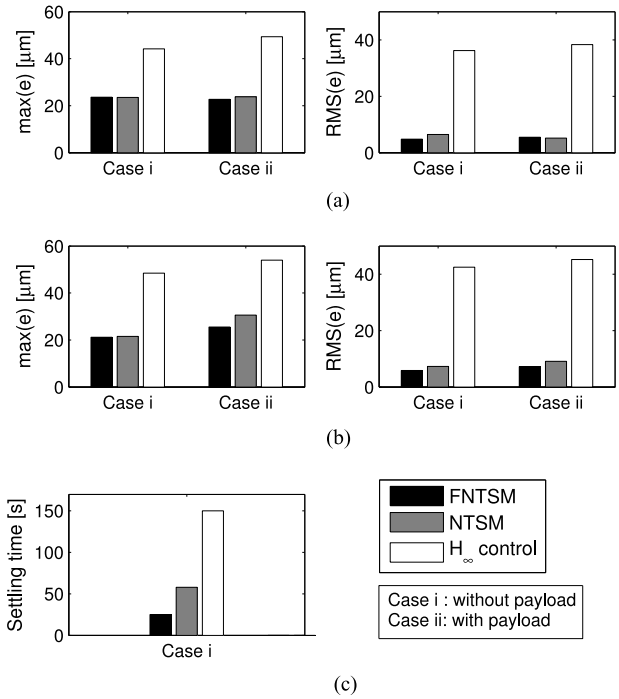

Fig. 10. Summary and comparison of the experimental results. (a) Swept sinusoidal tracking; (b) slope-varying triangular tracking; (c) disturbance rejection.

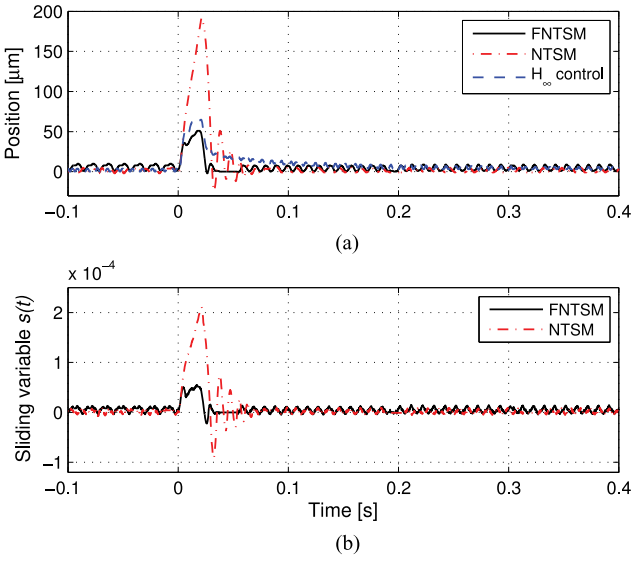

Fig. 9. Tracking responses to an external shock disturbance. (a) Position profiles; (b) Trajectories of sliding variable $s(t)$.

C. Fast Rejection of External Disturbance

As we have discussed in Remark 3, comparing with the NTSM control, apart from the property of chattering free, the most important benefit the FNTSM control can provide is its faster convergence rate in response to an external disturbance. To verify this benefit, we carry out the experiments using a shock disturbance with a duration of 20 ms, which is acting on the LM stage periodically for easy observation. Fig. 9(a) shows the time responses under the three controllers. It is clear that the FNTSM control takes the least settling time with 25 ms for the position to converge within 10 μm. Comparatively, the NTSM control is disturbed with the largest error magnitude and takes 58 ms to settle down; while the H_∞ controller takes the longest time of 150 ms to settle due to its weakest robustness. Furthermore, the time trajectories of the sliding variables $s(t)$ are shown in Fig. 9(b), which also indicate the faster convergence rate achieved by the FNTSM control.

D. Summary and Comparison

The foregoing experimental results are summarized and compared in Fig. 10, where we also compare the root mean square (RMS) of the sampled tracking error $e(i)$ as defined by

$$\mathrm{RMS}(e) = \sqrt{\sum_{i=1}^{N} \frac{e^2(i)}{N}} \tag{39}$$

where N is the number of the samples. We can see that the FNTSM control achieves the smallest max(e) and RMS(e) in all cases. For the NTSM control, it obtains similar max(e) with the FNTSM control, but has larger RMS(e). Comparatively, the H_∞ control gets the worst performance, especially when with payload. Moreover, the FNTSM control has a significantly least settling time in rejecting the external disturbance as shown in Fig. 10(c). Therefore, the results evidently demonstrate that the FNTSM control can be easily implemented in practice, and also provides both stronger tracking robustness and faster response to disturbance rejection.

V. Conclusion

In this paper, we have developed a robust LM controller using FNTSM. In particular, the selection of the controller parameters are discussed by considering the unmodeled time delay associated with the LM dynamics, measurement noises, and the tradeoffs between robustness and tracking accuracy. We also present a velocity estimator, which is model free and is robust against the quantization noises in the position measurements. It is demonstrated that the FNTSM controller is easy to implement only with a small amount of control chattering, which is inevitably due to the measurement noises rather than the control law. Moreover, experimental results show that the FNTSM controller achieves better tracking accuracy and considerably faster disturbance rejection than the conventional NTSM controller and H_∞ controller. The superior performance is also retained under the payload variation. Therefore, the FNTSM control method is suitable for the applications, where the performance criteria with strong robustness, fast convergence rate, and easy implementation are all essential.

Appendix

Giving the following first-order nonlinear differential inequality

$$\dot{V}(x) + \alpha V(x) + \beta V^{\gamma}(x) \leq 0 \tag{40}$$

where $V(x)$ represents a positive Lyapunov function with respect to the state $x \in R$, $\alpha, \beta > 0$, and $0 < \gamma < 1$, then for any given initial condition $V(x(0)) = V_0$, the function $V(x)$ converges to the origin in the finite time as follows:

$$T \leq \frac{1}{\alpha(1-\gamma)} \ln \frac{\alpha V_0^{1-\gamma} + \beta}{\beta}. \tag{41}$$

See [27] and references therein for more details.

References

[1] N. C. Shieh, P. C. Tung, and C. L. Lin, "Robust output tracking control of a linear brushless DC motor with time-varying disturbances," *IEEE Proc. Electr. Power Appl.*, vol. 149, no. 1, pp. 39–45, Jan. 2002.

[2] A. T. Elfizy, G. M. Bone, and M. A. Elbestawi, "Model-based controller design for machine tool direct feed drives," *Int. J. Mach. Tools Manuf.*, vol. 44, pp. 465–477, 2004.

[3] M. A. Stephens, C. Manzie, and M. C. Good, "Model predictive control for reference tracking on an industrial machine tool servo drive," *IEEE Trans. Ind. Inf.*, vol. 9, no. 2, pp. 808–816, May 2013.

[4] J. Zheng and M. Fu, "Nonlinear feedback control of a dual-stage actuator system for reduced settling time," *IEEE Trans. Control Syst. Technol.*, vol. 16, no. 4, pp. 717–725, Jul. 2008.

[5] L. Lu, Z. Chen, B. Yao, and Q. Wang, "Desired compensation adaptive robust control of a linear-motor-driven precision industrial gantry with improved cogging force compensation," *IEEE/ASME Trans. Mechatronics*, vol. 13, no. 6, pp. 617–624, Dec. 2008.

[6] Z. Z. Liu, F. L. Luo, and M. A. Rahman, "Robust and precision motion control system of linear-motor direct-drive for high speed X-Y table positioning mechanism," *IEEE Trans. Ind. Electron.*, vol. 52, no. 5, pp. 1357–1363, Oct. 2005.

[7] S. W. Youn, J. J. Lee, H. S. Yoon, and C. S. Koh, "A new cogging-free permanent-magnet linear motor," *IEEE Trans. Magn.*, vol. 44, no. 7, pp. 1785–1790, Jul. 2008.

[8] K. Sato, M. Katori, and A. Shimokohbe, "Ultrahigh-acceleration moving-permanent-magnet linear synchronous motor with a long working range," *IEEE/ASME Trans. Mechatronics*, vol. 18, no. 1, pp. 307–315, Feb. 2013.

[9] S.-L. Chen, K. K. Tan, S. Huang, and C. S. Teo, "Modeling and compensation of ripples and friction in permanent-magnet linear motor using a hysteretic relay," *IEEE/ASME Trans. Mechatronics*, vol. 15, no. 4, pp. 586–584, Aug. 2010.

[10] H. Fujimoto and B. Yao, "Multirate adaptive robust control for discrete time non-minimum phase systems and application to linear motors," *IEEE/ASME Trans. Mechatronics*, vol. 10, no. 4, pp. 371–377, Aug. 2005.

[11] M. Butcher and A. Karimi, "Linear parameter-varying iterative learning control with application to a linear motor system," *IEEE/ASME Trans. Mechatronics*, vol. 15, no. 3, pp. 412–420, Jun. 2010.

[12] J. Zheng, W. Su, and M. Fu, "Dual-stage actuator control design using a doubly coprime factorization approach," *IEEE/ASME Trans. Mechatronics*, vol. 15, no. 3, pp. 339–348, Jun. 2010.

[13] V. I. Utkin, "Sliding mode control design principles and applications to electric drives," *IEEE Trans. Ind. Electron.*, vol. 40, no. 1, pp. 23–36, Feb. 1993.

[14] Y.-F. Li and J. Wikander, "Model reference discrete-time sliding mode control of linear motor precision servo systems," *Mechatronics*, vol. 14, no. 7, pp. 835–851, Sep. 2004.

[15] F.-J. Lin, P.-H. Chou, C.-S. Chen, and Y.-S. Lin, "DSP-based cross-coupled synchronous control for dual linear motors via intelligent complementary sliding mode control," *IEEE Trans. Ind. Electron.*, vol. 59, no. 2, pp. 1061–1073, Feb. 2012.

[16] J. E. Slotine and W. Li, *Applied Nonlinear Control*. Englewood Cliffs, NJ, USA: Prentice-Hall, 1991.

[17] Q. Hu, C. Du, L. Xie, and Y. Wang, "Discrete-time sliding mode control with time-varying surface for hard disk drives," *IEEE Trans. Contr. Syst. Technol.*, vol. 17, no. 1, pp. 175–183, Jan. 2009.

[18] S. Li, M. Zhou, and X. Yu, "Design and implementation of terminal sliding mode control method for PMSM speed regulation system," *IEEE Trans. Ind. Inf.*, vol. 9, no. 4, pp. 1879–1891, Nov. 2013.

[19] H. Wang, H. Kang, Z. Man, D. M. Tuan, Z. Cao, and W. Shen, "Sliding mode control for steer-by-wire systems with AC motors in road vehicles," *IEEE Trans. Ind. Electron.*, vol. 61, no. 3, pp. 1596–1611, Mar. 2014.

[20] E. D. Engeberg and S. G. Meek, "Adaptive sliding mode control for prosthetic hands to simultaneously prevent slip and minimize deformation of grasped objects," *IEEE/ASME Trans. Mechatronics*, vol. 18, no. 1, pp. 376–385, Feb. 2013.

[21] V. I. Utkin, *Sliding Modes in Control and Optimization.* New York, NY, USA: Springer-Verlag, 1992.

[22] B. Bandyopadhyay, S. Janardhanan, and S. K. Spurgeon, *Advances in Sliding Mode Control: Concept, Theory and Implementation* (Lecture Notes in Control and Information Sciences), vol. 440. Berlin, Germany: Springer, 2013.

[23] Z. Man and X. Yu, "Terminal sliding mode control of MIMO systems," *IEEE Trans. Circuits Syst. I, Fundam. Theory Appl*, vol. 44, no. 11, pp. 1065–1070, Nov. 1997.

[24] K. Abidi, J.-X. Xu, and J.-H. She, "A discrete-time terminal sliding-mode control approach applied to a motion control problem," *IEEE Trans. Ind. Electron.*, vol. 56, no. 9, pp. 3619–3627, Sep. 2009.

[25] Y. Feng, X. Yu, and Z. Man, "Non-singular terminal sliding control of rigid manipulators," *Automatica*, vol. 38, no. 12, pp. 2159–2167, Dec. 2002.

[26] V. I. Utkin and A. S. Poznyak, "Adaptive sliding mode control with application to super-twist algorithm: Equivalent control method," *Automatica*, vol. 49, no. 1, pp. 39–47, Jan. 2013.

[27] S. Yu, X. Yu, B. Shirinzadeh, and Z. Man, "Continuous finite-time control for robotic manipulators with terminal sliding mode," *Automatica*, vol. 41, no. 11, pp. 1957–1964, Nov. 2005.

[28] X. Yu and Z. Man, "Fast terminal sliding-mode control design for nonlinear dynamical systems," *IEEE Trans. Circuits Syst. I, Fundam. Theory Appl*, vol. 49, no. 2, pp. 261–264, Feb. 2002.

[29] A. Levant, "Robust exact differentiation via sliding mode technique," *Automatica*, vol. 34, no. 3, pp. 379–384, Mar. 1998.

[30] J. Zheng and M. Fu, "A reset state estimator using an accelerometer for enhanced motion control with sensor quantization," *IEEE Trans. Control Syst. Technol.*, vol. 18, no. 1, pp. 79–90, Jan. 2010.

[31] V. T. Haimo, "Finite time controllers," *SIAM J. Control Optim.*, vol. 24, no. 4, pp. 760–770, Jul. 1986.

[32] Y. Hong, J. Huang, and Y. Xu, "On an output finite-time stabilization problem," *IEEE Trans. Autom. Control*, vol. 46, no. 2, pp. 305–309, Feb. 2001.

[33] D. Simon, *Optimal State Estimation*. Hoboken, NJ, USA: Wiley, 2006.

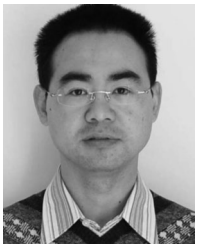

Jinchuan Zheng (M'13) received the B.Eng. and M.Eng. degrees in mechatronics engineering from Shanghai Jiao Tong University, Shanghai, China, in 1999 and 2002, respectively, and the Ph.D. degree in electrical and electronic engineering from Nanyang Technological University, Singapore, in 2006.

In 2005, he joined the Australian Research Council Centre of Excellence for Complex Dynamic Systems and Control, School of Electrical and Computer Engineering, University of Newcastle, Newcastle, Australia, as a Research Academic. From 2011 to 2012, he worked as a Staff Engineer at Western Digital Hard Disk Drive R&D Center, Singapore. He is currently a Lecturer at Swinburne University of Technology, Melbourne, Australia. His research interests include mechanism design and control of high precision mechatronic systems, sensing and vibration analysis, dual-stage actuation, and vision-based control.

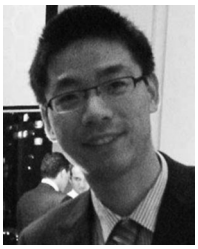

Hai Wang (M'13) received the B.E. degree from Hebei Polytechnic University, Tangshan, China, in 2007, the M.E. degree from Guizhou University, Guiyang, China, in 2010, and the Ph.D. degree from the Swinburne University of Technology, Melbourne, Australia, in 2013, all in electrical and electronic engineering.

He is currently with the Faculty of Science, Engineering and Technology, Swinburne University of Technology. His research interests are in sliding mode control, adaptive control, robotics, neural networks, nonlinear systems, and vehicle dynamics and control.

Zhihong Man (M'94) received the B.E. degree from Shanghai Jiao Tong University, Shanghai, China, in 1982, the M.Sc. degree from the Chinese Academy of Sciences, Beijing, China, in 1987, and the Ph.D. degree from the University of Melbourne, Melbourne, Australia, in 1994, respectively.

From 1994 to 1996, he was the Lecturer in the School of Engineering, Edith Cowan University, Joondalup, Australia. From 1996 to 2001, he was the Lecturer, and then, the Senior Lecturer in the School of Engineering, University of Tasmania, Hobart, Australia. From 2002 to 2007, he was the Associate Professor of Computer Engineering at Nanyang Technological University, Singapore. From 2007 to 2008, he was the Professor and the Head of Electrical and Computer Systems Engineering, Monash University Sunway Campus, Malaysia. Since 2009, he has been with the Swinburne University of Technology, Melbourne, as the Professor in the Faculty of Science, Engineering and Technology. His research interests are in nonlinear control, signal processing, robotics, neural networks, and vehicle dynamics and control.

Jiong Jin (M'11) received the B.E. (First Class Hons.) degree in computer engineering from Nanyang Technological University, Singapore, in 2006, and the Ph.D. degree from the University of Melbourne, Melbourne, Australia, in 2011.

He is currently a Lecturer in the School of Software and Electrical Engineering, Faculty of Science, Engineering and Technology, Swinburne University of Technology, Melbourne. Prior to that, he was a Research Fellow in Department of Electrical and Electronic Engineering, University of Melbourne, from 2011 to 2013. His research interests include network design and optimization, nonlinear systems and sliding mode control, robotics, wireless sensor networks and Internet of things, cyber-physical systems and applications in smart grids and smart cities.

Minyue Fu (S'84–M'87–SM'94–F'02) received the Bachelor's Degree in electrical engineering from the University of Science and Technology of China, Hefei, China, in 1982, and the M.S. and Ph.D. degrees in electrical engineering from the University of Wisconsin-Madison, Madison, WI, USA, in 1983 and 1987, respectively.

From 1987 to 1989, he was an Assistant Professor in the Department of Electrical and Computer Engineering, Wayne State University, Detroit, MI, USA. He joined the Department of Electrical and Computer Engineering, University of Newcastle, Newcastle, Australia, in 1989. He has been the Head of the Department and the Head of the School. He is currently a Chair Professor in electrical engineering. In addition, he was a Visiting Associate Professor at the University of Iowa, Iowa, IA, USA, in 1995–1996, and a Senior Fellow/Visiting Professor at Nanyang Technological University, Singapore, in 2002. His main research interests include control systems, signal processing, and communications.

Dr. Fu has been an Associate Editor for the IEEE TRANSACTIONS ON AUTOMATIC CONTROL, AUTOMATICA and *Journal of Optimization and Engineering*.